Decadal variability of summer Southern African rainfall

Bastien Dieppois[1, 2, 3], Benjamin Pohl[4], Mathieu Rouault[2, 5], Mark New[2], Noel Keenlyside[6], Damian Lawler[1]

[1] Centre for Agroecology, Water and Resilience, Coventry University, UK.
[2] African Climate and Development Initiative, University of Cape Town, RSA.
[3] Department of Oceanography, MARE Insitute, University of Cape Town, RSA.
[4] Centre de Recherche de Climatologie, Université de Bourgogne, France
[5] Nansen-Tutu Center for Marine Environmental Research, University of Cape Town, RSA.
[6] Geophysical Institute, University of Bergen and Bjerknes Centre for Climate Research, Norway.

Abstract – Summer Southern African rainfall exhibit three significant timescales of variability over the 20th century: interdecadal (15–28 year), quasi-decadal (8–13 year) and interannual (2–8 year). Teleconnections with global sea-surface temperature and atmospheric circulation anomalies are different for each timescale. Interdecadal fluctuations in summer rainfalll are associated with the Pacific Decadal Oscillation (PDO), while quasi-decadal and interannual fluctuations are related to decadal ENSO-like, often described as the Interdecadal Pacific Oscillation (IPO), and ENSO. Annular geopotential anomalies related the Pacific SST influence strongly interact with those driven by the Southern Annular Mode (SAM). Shifts in the westerlies thus lead to anomalous low-level easterly moisture fluxes from the Mascarene region even though decadal timescales, which are not significantly expressed in the SAM.

1. Introduction

Year-to-year variations in rainfall across Southern Africa have major consequences for human livehoods and ecosystems through their impact on drought, temperature, water supply, vegetation and agriculture. Interannual variability of summer Southern African rainfall is known to be primarily influenced by El Niño Southern Oscillation (ENSO), with dry/wet anomalies during El Niño/La Niña (e.g., Ropelewski and Halpert, 1987, Mason & Jury, 1997; Rouault & Richard, 2005).

Decadal fluctuations have also been found in summer Southern African rainfall (*e.g.,* Dyer & Tyson, 1977; Mason & Jury, 1997; Jury, 2014). Of particular importance is the interdecadal Dyer-Tyson cycle, which has been recently related to the SAM, and thus to changes in the meridional circulations (Malherbe *et al*., 2014). Also, a quasi-decadal cycle has been described as a chaotic resonance of high-frequency variability (Reason and Rouault, 2002). However, until now, discussions about potential mechanisms of these decadal fluctuations have been limited. For instance, most of the studies are based on comparisons between two periods of approximately 10-years, which are too short to capture the decadal signals (*i.e.*, roughly two ½ cycles). They are thus likely to describe changes in interannual variability between two decades that are not necessarily related to decadal signals. Using a time-scape approach based on spectral analysis, this study aims to address these gaps, by defining the changing characteristics of summer South African rainfall, and their specific teleconnections for the main timescale of climate variability.

2. Data

The Climatic Research Unit data set (CRU TS 3.22) is used to estimate Southern African rainfall from 1901 to 2013. The Summer Rainfall Index (SRI) has been defined by averaging the values over the regions where the wettest months occur between November and February (NDJF; red in Fig. 1a). We also used the multi-proxy summer Southern African rainfall reconstruction back to 1796 (Neukom et al., 2014).

To examine teleconnections with global SSTs, we used the monthly Sea-Surface Temperature (SST) data from the extended reconstructed SST (ERSST.v4) of the National Climatic Data Centre. To infer monthly atmospheric dynamics, the Twentieth Century Reanalysis version 2 (20CR.v2) is used.

3. Timescale of Summer Southern African rainfall variability

Timescales of summer Southern African rainfall variability are identified according to the global wavelet spectra (Fig. 1a). In observation, interannual (*i.e.*, 2–8 years), quasi-decadal (8–13 years; QDV) and interdecadal (15–28 year; IDV) timescales are significant and fairly spatially coherent (Fig. 1a). This is not true at the multidecadal scale (>30 year), where observations are constrained by edge, wrap-around and zero-padding effects. However, multidecadal fluctuations are significantly identified in the reconstruction from Neukom *et al*. (2014; Fig. 1a). At the first glance, a distinct separation (*i.e.*, spectral gap) between the interdecadal and quasi-decadal signals does not seem to be clear in the bicentennial reconstruction. But, according to the continuous wavelet spectra, these two timescales are only separated over the 20th century in the observed and reconstructed SRI (Fig. 1b-c). The SRIs display significant increasing variance since the 1930s at the interdecadal timescale, and since the late 1960s at the quasi-decadal timescale (Fig. 1b-c).

4. Multi-scale relationship with global SSTs

The teleconnections between the SRI and the global SSTs are examined using composite analysis (Fig. 2a-c). The time-series are subjected to a FFT filtering before to construct typical states of SSTs during periods of high-amplitude (*i.e.*, ≥ 1 standard deviation of interannual to interdecadal fluctuations) and for the successive timescales analyzed.

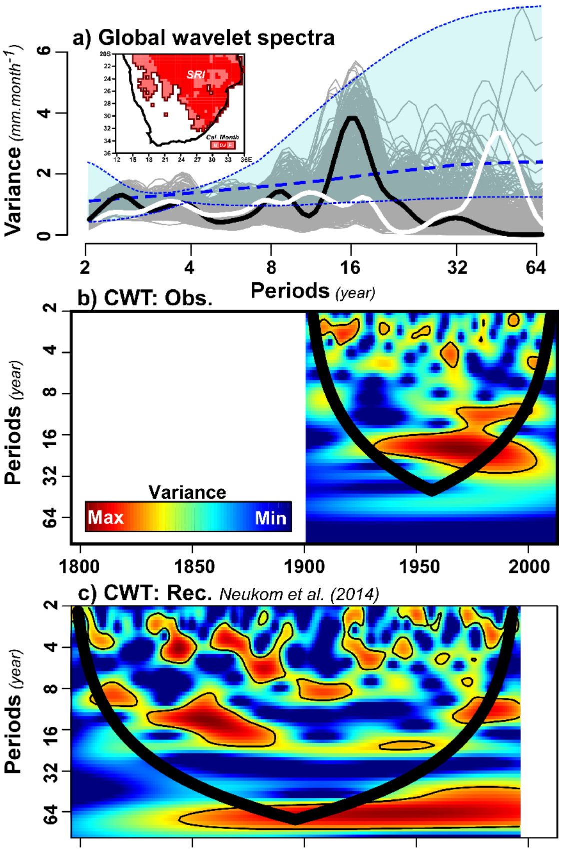

Figure 1. Timescale pattern of SRI variability (a) Global wavelet spectra of the observed SRI (black), of each grid-points used for its calculation (grey), and of the reconstructed SRI (white). The dashed blue lines indicate the red noise spectra with regard to the first order autoregressive of the observed SRI and its potential spatial drifts (b-c) Continuous wavelet spectrum of the observed and reconstructed SRI. Bold lines delineate the area under which power can be underestimated as a consequence of zero padding; thin contour lines show the 95% confidence limits based on Monte-Carlo simulations of the red noise background spectrum.

At the interdecadal timescale (15–28 year; IDV), Pacific SST anomalies associated with positive SRI display a horseshoe pattern, with cold anomalies in the central North Pacific surrounded by anomalies of opposite sign east of Asia, off California, in the Alaska gyre and in Southern Hemisphere extratropical regions (Fig. 2a). This SST pattern is consistent with the interdecadal signals described by Tourre *et al.* (2001), and it is also reminiscent of the Pacific Decadal Oscillation (PDO) during its negative phase (Mantua *et al*., 1997).

At the quasi-decadal timescales (8–13 year; QDV), Pacific SST anomalies associated with positive SRI fluctuations show cold anomalies in the tropical Pacific flanked by a horseshoe pattern of opposite sign, with marked anomalies in both North and South Pacific (Fig. 2b). This SST pattern is consistent with the quasi-decadal signals described by Tourre et al. (2001), and is reminiscent of the Interdecadal Pacific Oscillation (IPO), which is a wide-basin pattern of ENSO, during its negative life-cycles (Power *et al.*, 1999). This negative IPO occurs concomitantly with cold anomalies in the tropical Indian Ocean, while the South Atlantic SST dipole is identified (Fig. 2b). However, note that the physical independence between the IPO and ENSO remains controversial (*e.g.*, Power *et al.*, 1999; Tourre *et al.*, 2001). The IPO might thus be viewed as a decadal ENSO-like.

At the interannual scale (2–8 year), Klein *et al.* (1999) suggest that La Niña SST anomalies, which are associated with a cooler tropical Indian Ocean SST, are related to positive SRI anomalies (Fig. 2c).

5. Atmospheric circulation

Figure 2d-f displays composite anomalies of geopotential (z) and moisture fluxes at 1000 hPa based on significant timescales of SRI variability.

At the interdecadal timescale (15–28 year; IDV), low-tropospheric circulations associated with positive SRI display a quasi-annular mode, with low-pressure anomalies between the Polar Regions and 36°S and high-pressure anomalies in the subtropical and tropical regions (Fig. 2d). A southward shift of subtropical westerly moisture fluxes is identified for a large part of the Southern Hemisphere, which acts to weaken westerly moisture flows toward South Africa (Fig. 2d). This leads to an anomalous anticyclonic circulation in the Mascarene high-pressure region driving an anomalous low-level easterly flux along 10–20°S towards Southern Africa, which is favored by low-pressure anomalies over the continent (Fig. 2d). Such anomalies have some similarities with those driven by the Southern Annular Mode (SAM;

spatial correlation = 0.51), but there is no significant interdecadal signal in the summer SAM index (not shown). These geopotential anomalies are therefore unrelated to the SAM.

At the quasi-decadal timescale (15–28 year; QDV), positive SRI anomalies are associated with an annular signal in the Southern Hemisphere, with weak low-pressure anomalies over Antarctica and in the tropics over the Atlantic and Indian basins, as well as high-pressure anomalies in the mid-latitudes and tropical Pacific (Fig. 2e). Due to zonally asymmetric patterns in the annual geopotential anomalies between the Atlantic and the Indian Ocean, high-pressure anomalies are northward in the Indian Ocean up to Madagascar (Fig. 2e). An anomalous low-level easterly moisture flux reaching southeastern Africa is generated from enhancing the Mascarene High. These anomalies are partly reminiscent of those driven by the SAM and ENSO (spatial correlation = 0.48 and 0.53, respectively). However, there is significant quasi-decadal signal in different ENSO and IPO indices, but not in the SAM (not shown). Summer rainfall variability would thus be predominantly driven by the tropical dynamic linked to ENSO, the IPO or decadal ENSO-like.

At the interannual timescale (2-8 year), similar annular geopotential anomalies to those observed at the quasi-decadal scale are linked to positive SRI. Low-pressure anomalies in the Polar Regions and asymmetric enhancing of the St Helena and Mascarene Highs indicate a southward shift of the westerly wind belt (Fig. 2f). Meanwhile, anomalous low-level easterly moisture flux into South Africa, which is favored by low-pressure anomalies over the continent, is generated from anticyclonic circulation in the South Indian Ocean (Fig. 2f). These anomalies, even though they are weak over Antarctica and reveal some zonal asymmetries in the mid-latitudes, show some similarities with the SAM (spatial correlation = 0.58), but also with the Southern Oscillation Index (spatial correlation = 0.47). This is consistent with earlier studies (Pohl *et al.*, 2009), which show the statistical dependence between the SAM and ENSO in austral summer, and their consequences for Southern African rainfall.

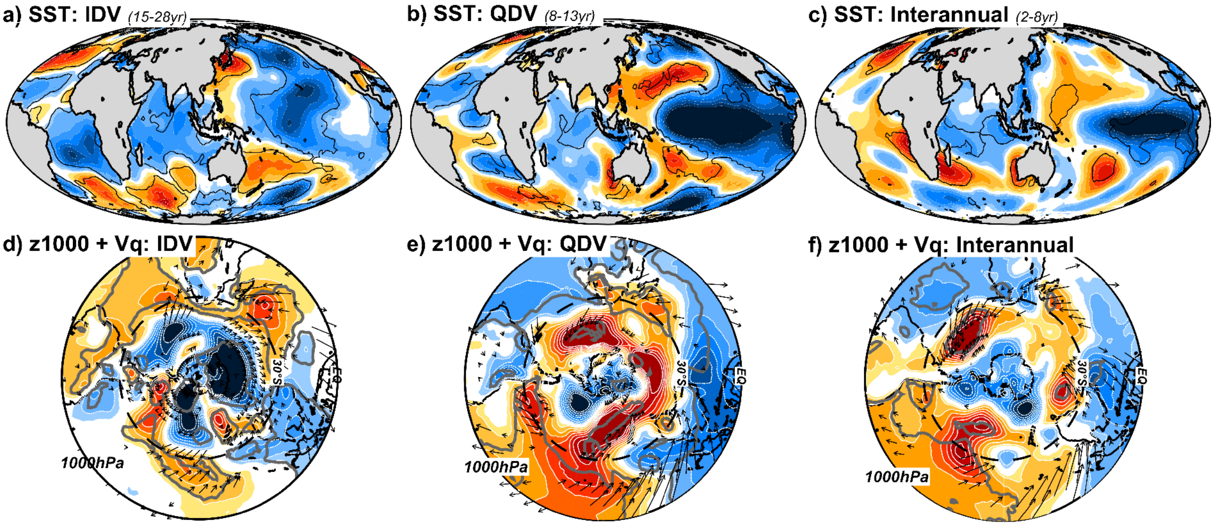

Figure 2. Summer anomalies of SSTs and low-tropospheric circulations associated with periods of high-amplitude over the dominant timescales of SRI variability. (a) Interdecadal composite anomalies of SSTs (in °C) during periods of enhancing interdecadal variability (IDV ≥ 1 standard deviation) in the SRI.(b-c) as for (a) but for the quasi-decadal and interannual timescale (QDV). (d-f) as for (a-c) but for geopotential height (z in m) and moisture fluxes (arrows, Vq in gkg^{-1}m.s^{-1}) at 1000 hPa. The statistical significance (contours) has been estimated by testing the difference in mean between geopotential height anomalies during periods of rainfall variability greater and lower than 1 SD, through a modified t-test accounting for pseudo-replication in the series at p=0.05. Only significant zonal and meridional moisture flux anomalies at p = 0.05 are shown by arrows.

6. Conclusion

This study analyses the changing characteristics of winter rainfall, and their teleconnections with large-scale climate through the dominant timescale of variability. As determined by wavelet analysis, observed and reconstructed summer rainfall exhibit three significant timescales of variability since the end of the 19th century: interdecadal, quasi-decadal and interannual. Summer Southern African rainfall displays significant increasing variance since the 1930s at the interdecadal timescale, and since the late 1960s at the quasi-decadal timescale. Multidecadal fluctuations can also be detected based on the reconstruction back to 1796, but, due to the shortness of the instrumental records, any study of multidecadal teleconnections is limited.

Teleconnections with global SST and atmospheric circulation anomalies are different on all three timescales considered here. As proposed by Dieppois *et al.* (2015), the PDO can drive interdecadal fluctuations in summer South African rainfall in shifting the Walker circulation and, at the regional scale, the South Indian Convergence Zone. Decadal ENSO-like (or the IPO) and ENSO also drive such anomalies, but at the quasi-decadal and interannual timescale. Annular geopotential anomalies, which could be related to the SAM or ENSO-like anomalies in the Southern Hemisphere (Pohl *et al*., 2009), influence interdecadal to interannual variability in summer rainfall through shifts in the westerlies, which generate an anomalous low-level easterly moisture flux from the Mascarene region. At the decadal timescales, the influence of the IPO or decadal ENSO-like could result from the generation of atmospheric Rossby waves. This is consistent with Tourre *et al.* (2001), which proposed that interannual to quasi-decadal fluctuations in the equatorial Pacific require coupled Rossby wave dynamics.

These results present, for the first time, analyses of atmospheric dynamics associated with global ocean-atmosphere modes of variability which influence, seasonally and regionally, vital Southern African rainfall receipts at the decadal timescales. Such analyses will help to understand recurrent space-time evolution of rainfall and drought patterns across this dry region.

References

Dieppois, B., Pohl, B., Rouault, M., New, M., Lawler, D., Keenlyside, N. (Submitted). Interannual to Interdecadal variability of winter and summer Southern African rainfall, and their teleconnections. *Clim Dyn.*

Dyer, T.G.T, Tyson, P.D. (1977). Estimating above and below normal rainfall periods over South Africa, 1972–2000. *J. Appl. Meteor.* **16:**145–147.

Jury, M.K. (2014). Factors contributing to a decadal oscillation in South African rainfall. *Theor. Appl. Climatol*. Published online:doi.10.1007/s00704-014-1165-4.

Klein, S.A., Soden, B.J., Lau, N.C. (1999). Remote sea surface variations during ENSO: evidence for a tropical atmospheric bridge. *J. Clim.* **12:**917–932.

Malherbe, J., Landman, W.A., Engelbrecht, F.A. (2014). The bi-decadal rainfall cycle, Southern Annular Mode and tropical cyclones over the Limpopo River Basin, southern Africa. *Clim. Dyn.* **42:**3121–3138.

Mantua, N.J., Hare, S.R., Zhang, Y., Wallace, J.M., Francis, R.C. (1997). A Pacific Interdecadal Climate Oscillation with Impacts on Salmon Production. *Bull. Amer. Meteor. Soc.* **78:**1069–1079.

Mason, S.J., and Jury, M. (1997). Climatic variability and change over the Southern Africa: a reflection on underlying processes. *Prog. Phys. Geo*. **21:**23–50.

Neukom, R., Nash, D.J., Endfield, G.H., Grab, S.W., Grove, C.A., Kelso, C., Vogel, C.H., Zinke, J. (2014). Multi-proxy summer and winter precipitation reconstruction for southern Africa over the last 200 years. *Clim. Dyn.* **42:**2713–2726.

Pohl, B., Fauchereau, N., Richard, Y., Rouault, M., Reason, C.J.C. (2009). Interactions between synoptic, intraseasonal and Interannual convective variability over Southern Africa. *Clim. Dyn.* **33:**1033–1050.

Power, S., Casey, T., Folland, C.K., Colman, A., Mehta, V. (1999) Inter-decadal modulation of the impact of ENSO on Australia. *Clim. Dyn.* **15:**319–323.

Reason, C.J.C, Rouault, M. (2002). ENSO-like decadal patterns and South Africa rainfall. *Geophys. Res. Lett.* **29:**161–164.

Ropelewski, C.F., and Halpert, M.S. (1987). Global and regional scale precipitation patterns associated with the El Niño/Southern Oscillation. *Mon. Wea. Rev.* **115:**1606–1626.

Rouault, M., and Richard, Y. (2005). Intensity and spatial extent of droughts in Southern Africa. *Geophys. Res. Lett.* **32:**L15702.

Tourre, Y.M., Rajagopalan, B., Kushnir, Y., Barlow, M., White, W.B. (2001) Patterns of coherent ocean decadal and interdecadal climate signals in the Pacific basin during the 20th century. *Geophys. Res. Lett.* **28:**2069–2072.